Journal of Bangladesh Institute of Planners ISSN 2075-9363
Vol. 13, 2020 (Printed in June 2021), pp. 153-167, © Bangladesh Institute of Planners

Exploring the effect of biophysical composition on land surface temperature to identify urban heat clusters using remote sensing technique: A case study on Dhaka city, Bangladesh

Md. Hamidur Rahman[*]
Torit Chakraborty[**]
Md. Shaharier Alam[***]

Abstract

Rapid urbanization and changes in land use land cover (LULC) have affected the thermal character of cities across the globe. Researchers found that Remote Sensing (RS) based urban biophysical composition- vegetation coverage, built-up area coverage, impervious surface coverage, soil fractions can significantly explain land surface temperature (LST) variation both at a local and regional scale. Taking Dhaka City, Bangladesh, as an example, this study aimed at exploring the effect of biophysical composition on LST in the year 2020 and find out Urban Heat Island (UHI) clusters with different LST setting using spatial autocorrelation technique. We found that LST presented a significant positive correlation with Normalized Difference Built-up Index (NDBI), road percentage, and negative correlation with Normalized Difference Vegetation Index (NDVI), Normalised Difference Water Index (NDWI), Normalised Difference Bareness Index (NDBaI), porosity, water percentage, open space percentage. Further, the study conducted local Moran's *I* and Hot Spots (Getis-Ord-Gi statistics) analysis to find out the location of UHI clusters. Findings showed that 34 % of neighborhoods fall within one of the four spatial patterns of UHI clusters. Study findings would help urban planners and policymakers to have cogent understating on the relationship between urban thermal behavior, and its surface biophysical composition at fine spatial scales and hopes to provide a valuable reference for community planning, resource allocation, and sustainable development.

Keywords: land surface temperature; urban heat island; biophysical composition; landsat-8

1. Introduction

The temperature rise and its impact on the natural and human system has become a significant concern and topic of discussion for the researchers all around the world (Masson-Delmotte et al., 2018). Although urban area covers only three percent of the total earth surface, the urbanization process is happening very fast, and it has been predicted that, by 2030, more than 5.87 million square kilometers new area will be transformed into urban area globally (Seto et al., 2012).

Dhaka, being the capital city of a developing country, Bangladesh, facing a rapid transformation in urbanization patterns to manage increasing urban population and

[*] GIS Assistant, Asian Disaster Preparedness Center (ADPC), Dhaka-1206, Bangladesh, Email: rahman.sumon.buet@gmail.com

[**] Assistant Urban Planner, Asian Disaster Preparedness Center (ADPC), Dhaka-1206, Bangladesh; Email: toritchakraborty@gmail.com

[***] Assistant Urban Planner, Asian Disaster Preparedness Center (ADPC), Dhaka-1206, Bangladesh; Email: shaharier3@gmail.com

economic pressure (World Bank, 2007; Ahmed et al., 2013; Rahman, 2020). The rapid urban expansions have triggered a reduction of urban green space, where the natural surface is being converted into impervious ones (Dewan and Corner, 2013). Extensive change in natural surfaces is a significant cause of increasing land surface temperature (LST) and the development of urban heat islands (UHI) (Trotter et al., 2017), which is a condition where urban atmospheric and surface temperature is significantly higher than its peripheral rural regions (Kamruzzaman et al., 2018). However, the government and city officials in developing counties are poorly equipped to comprehend the need to consider heat extreme as a disaster, and thus efforts are merely taken to analyze heat events at the city scale. Therefore, studying the LST and the influential factors that stimulated the rise of temperature is crucial for the cities of developing countries.

UHIs have a significant impact on society, including a rise in heat-related mortality in many countries worldwide (Pascaline & Rowena, 2018). Socially vulnerable and depressed groups in urban areas, including the young and elderly population class, individuals with a disability and chronic diseases, and the urban poor, are predominantly exposed to extreme heat events (Uejio et al., 2011; Oleson et al., 2015). The extent of the built environment, population size and density, anthropogenic activity, and socio-economic aspects of a city play a critical role in determining the effect of urbanization on temperature variation (Tam et al., 2015; Chen et al., 2006). Considering that Dhaka has been experiencing significant natural space, i.e., wetland, green space reduction over the last few decades, it is necessary to understand underlying factors that are influencing heat island formation (Trotter et al., 2017; Dewan and Corner, 2013).

Urban land surface temperature derivation through remotely sensed imagery could be the alternative of traditional weather station based urban thermal environmental study (Gallo and Owen, 1999; Trotter et al., 2017). Especially for developing cities like Dhaka City, where a continuous thermal environment monitoring system through mobile or weather stations in multiple parts of the city is unavailable (Yow, 2007; Trotter et al., 2017). To investigate the relation between LULC and LST, one popular approach is to extract biophysical parameters through the use of indices that quantitatively represent LULC (Sun et al., 2012). The most common biophysical components used by researchers for the LST study include, i.e., Normalized Difference Vegetation Index (NDVI) to estimate the percent vegetation cover (Dewan and Yamaguchi, 2009; Huete et al., 2002), Normalized Difference Built-up Index (NDBI) as an indicator of built-up urban surfaces (Zha et al., 2003); Normalised Difference Bareness Index (NDBaI) as an indicator of bare soil surfaces (Zhao and Chen, 2005), and the Normalised Difference Water Index (NDWI) as an indicator of water-bodies and rivers (Sun et al., 2012); Land Surface Water Index (LSWI), porosity level (Kamruzzaman et al., 2018), land use percentages (Sannigrahi et al., 2018), etc. These indices are considered as the influential factors behind the urban thermal environment (Chen et al., 2006), and either positively or negatively impact the land surface temperature of an area (Weng and Yang , 2004; Li et al., 2009).

Several studies were conducted to find out the association between different biophysical components and LST (Sannigrahi et al., 2018; Guo et al., 2020; Firozjaei et al., 2019; Ghosh et al., 2019; Ishola, 2016). Similarly, in Bangladesh, many researchers investigated the association between LST and LULC change (Roy et al., 2020; Islam et al., 2019); the relation between spatial growth and LST (Rahman et al., 2020); prediction of future LST

from LULC model (Ahmed et al., 2013); LULC change (Dewan and Yamaguchi, 2009). However, almost all of the studies have provided city-wide results instead of on disaggregating the output at a finer geographic scale, i.e., UHI effect at the local administrative level. But these research outputs should reach policy makers and planners so that city development authority can take effective urban management techniques to predict LST accurately and mitigate the negative impact of UHI.

In light of the above-mentioned research gap, the objective of this research is to- (a) quantify biophysical parameters using remote sensing techniques; (b) quantify the association between biophysical parameters and land surface temperature (LST); (c) to identify UHI clusters with the different land surface temperature setting. Findings from this study would develop a deep understanding of the interaction effects of LST and biophysical parameters. Neighborhood specific results would provide an effective way of monitoring and assessing the urban thermal environment of the city.

2. Data and Method

2.1 Study area selection

Dhaka, the capital city of Bangladesh, one of the fastest-growing megacities in the world, has been selected as a case study area (Dewan and Yamaguchi, 2009). Dhaka has experienced rapid urban population growth, which led to a significant decline in urban green space and the conversion of the natural surface to impervious ones (Trotter et al., 2017). Hence, the urban surface temperature is becoming increasingly warmer than its natural surroundings (Ahmed et al., 2013). Dhaka Metropolitan (DMA) area, as defined by the City Development Authority, Rajuk, is the study extent for LST derivation. The study area covers approximately 304 Sq. Km., where more than 16 million people reside (Ahmed et al., 2013. Due to both vertical and horizontal expansion, the urban area is experiencing increased surface temperature over the year (Ahmed et al., 2013). It undergoes a humid, hot, and wet subtropical climate with an annual mean temperature of 26.1 °C, where March to May is in dry summer seasons (Rashid, 1978).

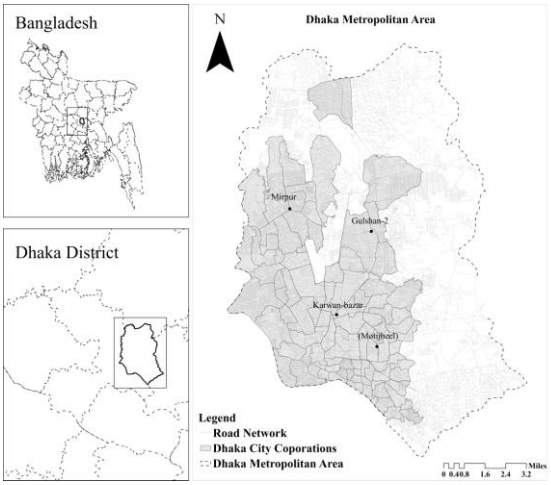

Source: Capital Development Authority, RAJUK; Map prepared by Author, 2020

Figure 1: Location of Dhaka Metropolitan Area (DMA)

2.2 Data description

The study used a multi-spectral satellite image of Landsat- 8, collected from the United States Geological Survey (USGS) database. Land use and land cover (LULC) maps, as well as the land surface temperature (LST) of the study area, have been derived using this satellite image. While selecting Landsat images, scene cloud coverage was set to less than 10% to get cloud-free images. Acquired images are Level-1T products. Hence, the image was both geometrically and radiometrically corrected, and therefore, didn't require any additional image preprocessing. The image has been projected to Universal Transverse Mercator (UTM) projection (within Zone 46 North), where the World Geodetic System (WGS)—1984 was used for the datum. Detail information on satellite image has been provided in Table 1.

Table 1: Satellite image information used for the study

Satellite	Sensor	Path/Row	Multi-Spectral band Resolution (m)	Thermal Band Resolution	Date (time)	Sun (Angle, Zenith)	Scene Cloud Cover
Landsat 8	OLI_TIRS	(p.137,r. 44)	30	100 m (resampled to 30 m)	March 30, 2020 (16:24:26)	(125.22, 59.470)	Less than 5% (0.93)

Source: Image courtesy of the U.S. Geological Survey, 2020

2.3 Method

2.3.1 Derivation of land cover maps

The Landsat-8 image was used to classify the LULC. The supervised Support Vector Machine (SVM) was used to classify the image in four categories which were- built-up, vegetation, water body, and bare soil. SVM was found as a better classifier by comparing it with other classifiers based on the accuracy-test (Kamruzzaman et al., 2018; Chakraborty et al., 2019). Moreover, SVM has a better performance for its low sensitivity to size, quality of training data, data distribution (Kamruzzaman et al., 2018). Most importantly, it can perform much better in the case of mixed pixels or wrong pixels for training data (Paneque-galvev et al., 2013).

Table 2: Description of land cover categories

Land cover types	Description
Built-up	Contains all infrastructure-residential, commercial, industrial, mixed-use, transportation network, pavements, man-made structures, etc.
Vegetation	Contains agricultural land, crop field, tree, park and playground, grassland, vegetated land, etc. land cover types.
Water Body	Contains river, wetlands (permanent/seasonal), lakes, ponds, canals, low-lying areas, etc.
Bare Soil	Contain vacant sites, sand-filled sites, construction sites, bare soils, excavation sites, open space, and remaining land cover types.

Source: Ahmed et al., 2013

The classification accuracy was performed in a multi-stage process. At first, 110 random points were generated in ArcGIS, and then the classified LULC information was stored into the point shape file. After that, those points were converted into the KMZ file for each LULC categories. The KMZ files then opened in Google Earth and overlaid on the high-resolution earth image. The accuracy of each point was then observed and stored in the same file. Finally, user accuracy, producer accuracy, overall accuracy, and kappa statistics were calculated using Excel and Python. The results showed that the SVM performed exceptionally well to classify the LULC with 90.9% of overall accuracy and 87.04% of the kappa score. It was also observed in producer accuracy built-up area had 97% accuracy. On the other hand, water had 84.6% accuracy.

Table 3: Accuracy assessment land cover types (confusion matrix)

Year	Land Cover Class	Accuracy (%)			
		Overall Accuracy	Kappa	Omission error (User's Accuracy)	Commission error (Producer's Accuracy)
2020	Built-Up	90.9	0.87	88.9	88.9
	Vegetation			90.0	90.0
	Water Body			91.7	91.7
	Bare Soil			93.3	93.3

Source: Author, 2020

2.3.2 Derivation of the Land Surface Temperature (LST) from Landsat 8 OLI image

For deriving the LST, the thermal band of Landsat 8, which are band 10 & 11, have been used. The following steps have been followed to derive LST-

First, Conversion of DN values into a meaningful radiance has been made using (Eq.1) (Chen et al., 2006; Ahmed et al., 2013).

$$L_\lambda = M_L \times Q_{cal} + A_L \quad (1)$$

Where, L_λ = TOA spectral radiance (Watts/ (m2×sr ×µm)); M_L = band Specific multiplicative rescaling factor from the metadata; A_L= Band Specific Multiplicative rescaling factor from the metadata; Q_{cal} = Quantized and calibrated standard product pixel values (DN)

Secondly, conversion from at-satellite radiances to at-sensor brightness temperatures has been made using the following Eq. 2 (Kamruzzaman et al., 2018; Li et al., 2016)

$$T_b = \frac{K_2}{\ln\left(\frac{K_1}{L_\lambda} + 1\right)} \quad (2)$$

Where,

T_b = TOA brightness temperature (in kelvin); K_1, K_2 are band Specific thermal conversion constant form the metadata; L_λ = TOA spectral radiance (Watts/ (m2×sr ×µm)). To get T_b in degree Celsius, 273.15 has been deducted.

Thirdly, fractional vegetation cover has been calculated using (Eq.3-4) (Deng and Wu, 2013)

$$\text{NDVI} = \left(\frac{Band5 - Band4}{Band5 + Band4}\right) \quad (3)$$

Where the range -1<NDVI<+1

After that, emissivity value has been assigned to pixels in terms of ranges of NDVI value-

The proportion of vegetation has been estimated using a maximum and minimum value of NDVI of the corresponding images by Eq. (4) (Deng and Wu, 2013).

$$\text{Pv} = \left(\frac{NDVI - NDVI_{min}}{NDVI_{max} - NDVI_{min}}\right)^2 \quad (4)$$

Fourthly, the land surface emissivity (LSE) has been calculated by the following (Eq.5) (Avdan and Jovanovska, 2016; Roy et al., 2014).

$$\text{LSE}(\varepsilon) = (0.004 * \text{Pv} + .986) \quad (5)$$

Finally, at-satellite brightness temperature has been converted to emissivity-corrected LST in degree Celsius using (Eq. 6) (Kamruzzaman et al., 2018; Li et al., 2016).

$$T_{LST} = \frac{T_b}{1 + \left[\left(\lambda \times \frac{T_b}{\alpha}\right) \ln(\varepsilon)\right]} \quad (6)$$

Where, λ = wavelength of the emitted radiance, 11.5 μm for TIRS Band 10; α = 14388 μ K, where α = hc/b (1.438×10^{-2}), here b = Boltzman constant as 1.38×10^{-23} J/K; h us the Plank's constant = 6.626×10^{-34} JS; c refers to the speed of light = 2.998×10^{8} m/s; ε = Surface emissivity

2.3.3 Derivation of biophysical parameters

The index-based biophysical parameters were found to be the best indicators of LST variations across space (Weng and Yang, 2004; Zhang et al., 2009). The NDVI, NDBI, NDWI, and NDBaI indices using Arc Map 10.3. The indices' expressions are as follows (Equation 7-10, respectively).

$$\text{NDVI} = \frac{(\text{Band 5}) - (\text{Band 4})}{(\text{Band 5}) + (\text{Band 4})} \quad (7) \qquad \text{NDBI} = \frac{(\text{Band 6}) - (\text{Band 5})}{(\text{Band 6}) + (\text{Band 5})} \quad (8)$$

$$\text{NDWI} = \frac{(\text{Band 5}) - (\text{Band 6})}{(\text{Band 5}) + (\text{Band 6})} \quad (9) \qquad \text{NDBaI} = \frac{(\text{Band 6}) - (\text{Band 10})}{(\text{Band 6}) + (\text{Band 10})} \quad (10)$$

The porosity level for 2020 has been calculated by using the ratio of non-built up areas to total areas for each neighborhood (Kamruzzaman et al., 2018). Here non-built up areas contain vegetation, water body, and bare soil land cover class. Likewise, road percentage, water body percentage, and open space area percentage have been calculated using zonal statistics tools of ArcGIS 10.6.

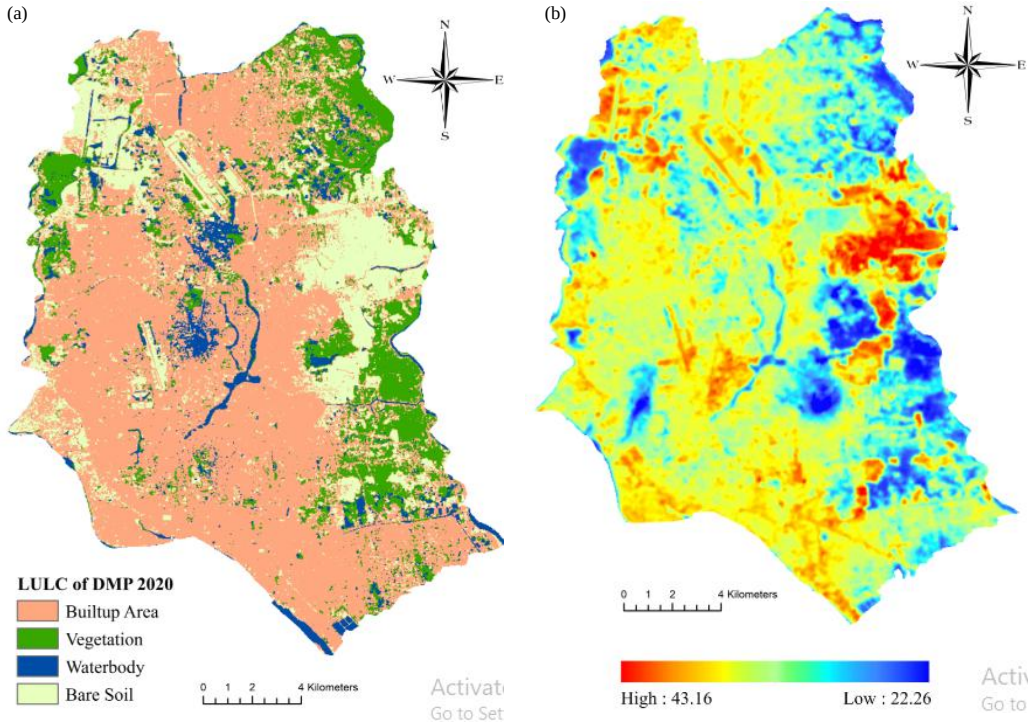

Source: Author, 2020

Figure 2: (a) Land cover map of DMA area 2020 (b) Land surface temperature map of DMA area 2020

3. Results

3.1 Land cover and land surface temperature (LST) distribution

Figure-2 (a) shows classified land cover map of DMA area where built-up areas cover 175.76 sq. km. (60.42 %) of total land, bare soil land areas cover 19.15 sq.km. (19.16 %), vegetation land areas cover 42.79 sq.km. (14.71 %), and water bodies cover 16.61 sq.km. (5.71%).

Figure-2 (b) shows the land surface temperature inside the DMA area. Visual comparison between Figures-2(a) and Figure-2(b), it can be observed that high LST areas are observed to be associated with built-up and bare-soil LULC classes, while areas of lower LST are associated with vegetation and water body.

Table 4: The variations of mean LST over different land cover types

LULC	Mean LST	STD
Built-up Area	34.69	2.09
Vegetation	30.51	2.45
Water body	31.77	2.37
Bare soil	33.41	2.65

Table-4 indicates that the built-up area has the highest mean LST value of 36.40°C, followed by bare soil land, which has a mean LST of 33.41°C. On the other hand, the water body and vegetation category show a comparatively lower mean LST value than the built-up and bare soil category. Vegetation and water body typically mitigate high surface temperatures due to differing albedos and heat storage capacity (Trotter et al., 2017).

Table 5: The ranges and descriptions of LST classifications

LST Category	Description	Area (Km^2)	Percentage (%)
(22.26-29.64) °C	Very Low LST Area	24.09	8.27
(29.64-32.75) °C	Low LST Areas	52.32	17.95
(32.75-35.05) °C	Moderate LST Areas	88.07	30.22
(35.05-37.59) °C	High LST Areas	100.88	34.61
(37.59-43.16) °C	Very High LST Areas	26.09	8.95

Source: Author, 2020

According to Table-5, a larger part of the DMA area (72%) fall within the moderate to very high-temperature zones. These findings are similar to the previous studies conducted in the DMA area. Ahmed et al., 2013 predicted that more than 56 % of areas of DMA would experience more than 30°C in 2019.

3.2 Factors affecting LST in the study area

Four land cover indices (e.g., NDVI, NDWI, NDBI, and NDBaI) were derived from satellite imagery data to quantify relationships between LST and the index. Besides, porosity, open space, and water body distribution level were calculated as it would define the amount of natural areas within a neighborhood, which would affect the UHI intensities (Kamruzzaman et al., 2018). As a physical development indicator, road network coverage data was incorporated. All these variables were calculated on the ward level of the DMA area using zonal statistics in ArcGIS.

Table 6: Descriptive statistics of biophysical parameters

Variables	***Min***	***Max***	***M***	***Std.***
Porosity	.682	23.21	7.73	4.82
% of Road	2.197	14.17	7.04	2.36
% of Open Space	.01	24.45	3.51	4.37
% of Water Body	.02	67.82	7.87	13.49
NDVI	-.212	-.617	-.176	.119
NDBI	-.629	.580	-.121	.128
NDWI	-.551	.271	-.164	.104
NDBaI	-.388	.215	-.046	.070

Source: Author, 2020

Table-6 shows that water body distribution has the highest standard deviation (13.49), which means there is a considerable variation in the distribution of water bodies in the study area. Similar findings can be observed for porosity and percentage of road variables. On the other hand, the land cover indices, i.e., NDVI, NDBI, NDWI, and NDBaI, has a significantly less variation in the distribution.

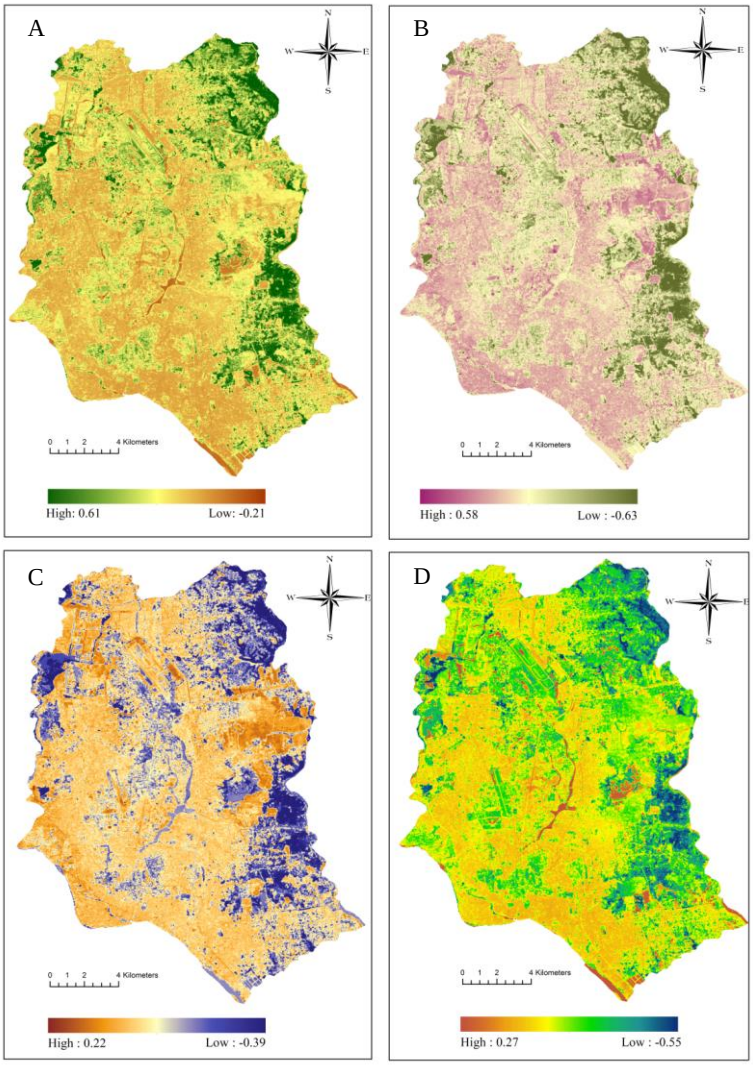

Source: Author, 2020

Figure 3: Spatial distribution of biophysical indices- (A) NDVI; (B) NDBI; (C) NDBaI; (D) NDWI in Dhaka Metropolitan Area

Table 7: Pearson's correlation coefficient the LST and the biophysical parameters

Variables	LST	NDVI	NDBaI	NDWI	NDBI	Porosity	*Road	*Water	*Open Space
LST	1								
NDVI	-0.59	1							
NDBaI	0.54	-0.89	1						
NDWI	-0.52	0.96	-0.85	1					
NDBI	0.54	0.91	-0.94	0.94	1				
Porosity	-0.43	0.72	-0.51	0.67	0.52	1			
Road	0.25	-0.55	0.54	-0.57	-0.55	-0.45	1		
Water	-0.14	0.14	-0.07	0.13	0.12	0.21	-0.149	1	
Open Space	-0.31	0.57	-0.36	0.63	0.50	0.69	-0.409	0.32	1

*indicated that variables are taken as a percentage of the total area in each administrative unit. (Source: Author, 2020)

The correlation matrix shows that LST presents a significant positive correlation with NDBI, road percentage (Table-7), and negative correlation with NDVI, NDWI, NDBaI, porosity, water percentage, open space percentage (Table-7).

3.3 LST clustering and Hotspots identification

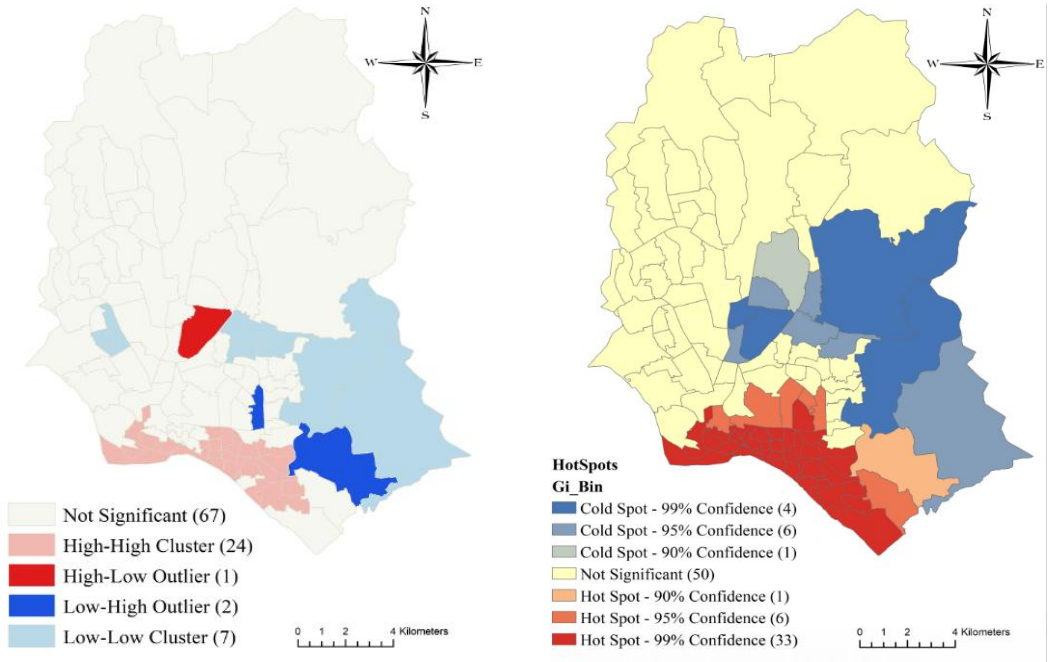

Source: Author, 2020

Figure 4: (A) Cluster and outlier analysis (Anselin Local Moran's I) result showing neighborhood location in different clusters of LST within DMA; (B) Hotspot analysis (Getis-Ord-Gi statistics) result showing neighborhoods with different statistically significant LST identified as hot spots and cold spots.

The LST objects that are located close to one another are more likely to have similar characteristics and geographic homogeneity, compared to those located farther from each other (Guo et al., 2020). Therefore, this study adopted a local Moran's I and Hot Spots (Getis-Ord-Gi statistics) tools to find out the location clusters of UHI. Figure-4 (A) indicated HH cluster as the LST object and its surroundings have a temperature concentration level significantly higher than the average level, suggesting UHI clusters from a central place; HL indicated that the LST object exhibits an obviously high concentration whereas the concentration of its neighboring objects is lower than average; HL indicated the LST object has a significantly low-level concentration, while the concentration levels of its surrounding objects are relatively high; LL means The temperature levels of both the LST object and its surroundings are somewhat lower than the average level of all objects.

3.4 Validation of identified UHI clusters

Table 8: Difference in biophysical parameters in different LST clusters

Clusters (Numbers)	Water-bodies (%)	Open Space (%)	Road Network (%)	Porosity	NDVI	NDBaI	NDWI	NDBI
HH (24)	7.85	3.01	8.15	2.95	0.08	-0.01	0.01	0.00
HL (1)	3.42	0.75	6.01	7.96	0.10	-0.02	0.01	0.00
LH (2)	65.60	15.83	4.52	9.78	0.15	-0.05	0.02	0.01
LL(7)	92.83	17.52	6.23	9.62	0.16	-0.04	0.03	0.02
NS (67)	36.62	8.71	6.83	9.19	0.13	-0.03	0.02	0.01

Source: Author, 2020

Biophysical parameter distribution can validate the result of the identified UHIs cluster. Table 8 shows that cluster wise variation in terms of biophysical parameter distribution. Higher physical development would reduce the previous land in an area; hence, contribute to land surface temperature increment. From Table-8, it can be seen that HH and HL neighborhoods have a high percentage of road network coverage, lower porosity level, lower percentage of water body areas, and open space compare to LH and LL neighborhoods. Moreover, in terms of LULC indices, HH and HL cluster have low mean NDVI, which means lower vegetation coverage, low mean NDWI suggests a lower amount of water body, low mean NDBI means a greater built-up area, etc.

4. Discussions and Conclusions

In this study, a comprehensive analysis has been conducted to find out the effect of biophysical characteristics on LST association with LULC. In addition, to investigate at the neighborhood level, the cluster analysis and hot spot analysis were performed by which the LST effect could be determined at the micro-level. During the last several decades, the urban thermal environment of Dhaka has significantly changed due to rapid LULC change through rapid urbanization (Trotter, et al., 2017). In relation to that, this research also found that the built-up area has 60.42% and 19.16 % of bare soil area in 2020. The highest mean LST was found in built-up (34.6°C) and bare soil (33.4°C) areas.

Several types of research also portrayed similar results where built-up and bare soil areas scored the highest LST mean value on different temporal variations (Ahmed et al., 2013; Weng, 2001; Weng and Yang, 2004). In comparison to the previous study of Ahmed et al., (2013), it is found that the built-up area has changed significantly from 36.91% in 2009 to 60.42% in 2020, a 23.51% area increase (63.69% change compared to base year, 2009). The same study also stated that bare soil area was 45.2%, whereas, this study found 19.16% of bare soil area in the DMA area. It can be assumed that over the decade, the bare soil area has converted to a built-up area due to the rapid urbanization process.

Based on the correlation output of this research, a negative association was observed between LST and NDVI, NDWI, porosity, percentage of water, percentage open space. The result is very contextual and significant as the LST value was found comparatively low, where the vegetation, water, and open space are relatively higher than other LULC. The same types of findings were observed in other studies. (Ahmed. et al., 2013; Trotter et al., 2017). On the contrary, NDBI, NDBaI, percentage of road found positively correlated with LST.

The study found major UHI cluster in southern part of the city which are wards Dhaka South City Corporation (DSCC), covering old part of the city. Physical development pattern of this area suggests high building floor space density (Rahman et al., 2019), along with intensive built-up land use (94%) (Rahman et al., 2020). While illustrating vertical growth condition of DMA, Rahman et al. (2020) found that mean building height of DNCC is higher than that of DSCC and Fringe areas of Dhaka. Due to lack of non-built up areas in core parts, city is growing horizontally in fringe areas, contributing to expansion of urban heat island boundary. Moreover, the mean LST value for summer season was found 36.5°C for DMA in 2014 (Rahman et al., 2020)., whereas, this study found mean LST as 37.3°C, which suggest an overall increase of .8 °C increase over only 6 year time period. Another finding is that areas located in the eastern part of the DMA area, i.e., Demra, Dakshingaon, Matuail, Saralia, Badda, Satarkul, Beriad, Dumni, etc. which are considered as fringe areas, have major land-use cover as agriculture, vegetation, and wetlands (Rahman et al., 2020). Assumable, these parts of the city have lower mean LST compare to the core city area. Hence, hot spots analysis results found that these areas are still in lower LST zones. However, for rapid urbanization, these areas are also loosing natural land cover more drastically; hence, they would continue to experience greater temperature in the near future.

To minimize the impact of UHI, growth control policy should be taken to balance and control the urbanization in the DMA area. The vertical expansion should be encouraged to control the horizontal growth, which will increase the impervious surface resulting in increasing LST. In addition to that, more open space, roadside plantation, lake, parks should be distributed very effectively to balance the impervious surface (built-up) ratio. In building level, green building, rooftop gardening should introduce. As the southern part of the study area is more vulnerable compare to the northern part so specific initiatives should be taken to minimize the extreme heat phenomenon. According to the research goal of this study, the findings should be incorporated to help the policymakers and urban planners to take necessary action to minimize the extreme heat effect of LST in the DMA area.

Previous studies have demonstrated that diurnal and seasonal variations exist between LST and land surface characteristics. Therefore, further studies that should address the temporal and spatial variation of the relationships between UHI and biophysical compositions.

References

Ahmed, B., Kamruzzaman, M., Zhu, X., Rahman, M., & Choi, K. (2013). Simulating land cover changes and their impacts on land surface temperature in Dhaka, Bangladesh. *Remote Sensing*, *5*(11), 5969-5998.

ArcGIS – GIS Software (Version 10.6). (2018). Redlands, California: Environmental Systems Research Institute (ESRI).

Avdan, U., Jovanovska, G., 2016. Algorithm for automated mapping of land surface temperature using LANDSAT 8 satellite data. *J. Sensors*, 2016.

Chakraborty, T., Alam, M. S., & Islam, M. D. (2019). Land Cover Classification from Multispectral Remote Sensing Image Using Deep Neural Network, K-Nearest Neighbor, Decision Tree and SVM Algorithms: A machine learning based comparison approach. Paper presented at 1st International Conference on Urban and Regional Planning-2019, Bangladesh, Bangladesh Institute of Planners, Dhaka, Bangladesh.

Chen, X. L., Zhao, H. M., Li, P. X., & Yin, Z. Y. (2006). Remote sensing image-based analysis of the relationship between urban heat island and land use/cover changes. *Remote sensing of environment*, *104*(2), 133-146.

Deng, C., Wu, C., 2013. Examining the impacts of urban biophysical compositions on surface urban heat island: a spectral unmixing and thermal mixing approach. *Remote Sens. Environ., 131*, 262 –274.

Dewan, A. M., & Yamaguchi, Y. (2009). Land use and land cover change in Greater Dhaka, Bangladesh: Using remote sensing to promote sustainable urbanization. *Applied geography*, *29*(3), 390-401.

Dewan, A., & Corner, R. (Eds.). (2013). *Dhaka megacity: Geospatial perspectives on urbanisation, environment and health*. Springer Science & Business Media.

Firozjaei, M. K., Alavipanah, S. K., Liu, H., Sedighi, A., Mijani, N., Kiavarz, M., & Weng, Q. (2019). A PCA–OLS Model for Assessing the Impact of Surface Biophysical Parameters on Land Surface Temperature Variations. *Remote Sensing*, *11*(18), 2094.

Gallo, K. P., & Owen, T. W. (1999). Satellite-based adjustments for the urban heat island temperature bias. *Journal of applied meteorology*, *38*(6), 806-813.

Ghosh, S., Chatterjee, N. D., & Dinda, S. (2019). Relation between urban biophysical composition and dynamics of land surface temperature in the Kolkata metropolitan area: a GIS and statistical based analysis for sustainable planning. *Modeling Earth Systems and Environment*, *5*(1), 307-329.

Guo, A., Yang, J., Xiao, X., Xia, J., Jin, C., & Li, X. (2020). Influences of urban spatial form on urban heat island effects at the community level in China. *Sustainable Cities and Society*, *53*, 101972.

Han-Qiu, X. U. (2005). A study on information extraction of water body with the modified normalized difference water index (MNDWI). *Journal of remote sensing*, *5*, 589-595.

Huete A, Didan K, Miura T, et al. (2002). Overview of the radiometric and biophysical performance of the MODIS vegetation indices. *Remote Sensing of Environment*, *83*(1-2): 195–213.

Ishola, K. A., Okogbue, E. C., & Adeyeri, O. E. (2016). Dynamics of surface urban biophysical compositions and its impact on land surface thermal field. *Modeling Earth Systems and Environment*, *2*(4), 1-20.

Islam, M. D., Chakraborty, T., Alam, M. S., & Islam, K. S. (2019). Urban heat island effect analysis using integrated geospatial techniques: A case study on Khulna city, Bangladesh. In International conference on climate change, Dhaka, Bangladesh.

Jiang, J., & Tian, G. (2010). Analysis of the impact of land use/land cover change on land surface temperature with remote sensing. *Procedia environmental sciences*, *2*, 571-575.

Kamruzzaman, M., Deilami, K., & Yigitcanlar, T. (2018). Investigating the urban heat island effect of transit oriented development in Brisbane. *Journal of Transport Geography*, *66*, 116-124.

Li, H., Liu, Q. H., & Zou, J. (2009). Relationships of LST to NDBI and NDVI in Changsha-Zhuzhou-Xiangtan area based on MODIS data. *Scientia Geographica Sinica*, *2*, 018.

Li, X., Li, W., Middel, A., Harlan, S.L., Brazel, A.J., Turner Ii, B.L. (2016). Remote sensing of the surface urban heat island and land architecture in Phoenix, Arizona: combined effects of land composition and configuration and cadastral –demographic –economic factors. Remote Sens. *Environ., 174*, 233 –243

Masson-Delmotte, V., Zhai, P., Pörtner, H. O., Roberts, D., Skea, J., Shukla, P. R., ... & Connors, S. (2018). Global warming of 1.5 C. *An IPCC Special Report on the impacts of global warming of*, *1*.

Mountrakis, G., Im, J., & Ogole, C. (2011). Support vector machines in remote sensing: A review. *ISPRS Journal of Photogrammetry and Remote Sensing*, *66*(3), 247-259.

Nurwanda, A., & Honjo, T. (2020). The prediction of city expansion and land surface temperature in Bogor City, Indonesia. *Sustainable Cities and Society*, *52*, 101772.

Oleson, K. W., Monaghan, A., Wilhelmi, O., Barlage, M., Brunsell, N., Feddema, J., ... & Steinhoff, D. F. (2015). Interactions between urbanization, heat stress, and climate change. *Climatic Change, 129*(3-4), 525-541.

Paneque-Gálvez, J., Mas, J. F., Moré, G., Cristóbal, J., Orta-Martínez, M., Luz, A. C., ... & Reyes-García, V. (2013). Enhanced land use/cover classification of heterogeneous tropical landscapes using support vector machines and textural homogeneity. *International Journal of Applied Earth Observation and Geoinformation*, *23*, 372-383.

Pascaline, W., & Rowena, H. (2018). Economic Losses, Poverty & Disasters: 1998-2017 [M]. *United Nations Office for Disaster Risk Reduction*.

Rahman, M. H. (2020). Does Neighborhood level Jobs-Housing Balance Associated with Work Purpose Commuting Time? : A Case Study on Dhaka City, Bangladesh. DOI: 10.13140/RG.2.2.27820.49284

Rahman, M., Avtar, R., Yunus, A. P., Dou, J., Misra, P., Takeuchi, W., ... & Kharrazi, A. (2020). Monitoring Effect of Spatial Growth on Land Surface Temperature in Dhaka. *Remote Sensing*, *12*(7), 1191.

Rahman, M. H., Islam, M., & Neema, M. N. (2019, January). *Compactness of Neighborhood Spatial Structure: A Case Study of Selected Neighborhoods of DNCC and DSCC Area*. Paper presented at International Conference on Sustainability in Natural and Built Environment (iCSNBE 2019), Dhaka, Bangladesh. Retrieved from http://www.icsnbe.net.au/proceedings/2019/iCSNBE2019_Proceedings.pdf

Rashid, H. (1978) Geography of Dhaka, In: Rashid, H, *Geography of Bangladesh*, 2 Eds., Dhaka: University Press, 78-94.

Roy, D.P., Wulder, M.A., Loveland, T.R., Woodcock, C.E., Allen, R.G., Anderson, M.C., Kennedy, R. (2014). Landsat-8: science and product vision for terrestrial global change research. Remote Sens. *Environ*. 145, 154–172.

Roy, S., Pandit, S., Eva, E. A., Bagmar, M. S. H., Papia, M., Banik, L., ... & Razi, M. A. (2020). Examining the nexus between land surface temperature and urban growth in Chattogram Metropolitan Area of Bangladesh using long term Landsat series data. *Urban Climate*, *32*, 100593.

Sannigrahi, S., Bhatt, S., Rahmat, S., Uniyal, B., Banerjee, S., Chakraborti, S., ... & Bhatt, A. (2018). Analyzing the role of biophysical compositions in minimizing urban land surface temperature and urban heating. *Urban climate*, *24*, 803-819.

Seto, K. C., Güneralp, B., & Hutyra, L. R. (2012). Global forecasts of urban expansion to 2030 and direct impacts on biodiversity and carbon pools. *Proceedings of the National Academy of Sciences*, *109*(40), 16083-16088.

Sun F, Sun W, Chen J, et al. (2012). Comparison and improvement of methods for identifying waterbodies in remotely sensed imagery. *International Journal of Remote Sensing*, 33(21): 6854-6875.

Sun, Q., Wu, Z., & Tan, J. (2012). The relationship between land surface temperature and land use/land cover in Guangzhou, China. *Environmental Earth Sciences*, *65*(6), 1687-1694.

Tam, B. Y., Gough, W. A., & Mohsin, T. (2015). The impact of urbanization and the urban heat island effect on day-to-day temperature variation. *Urban Climate*, *12*, 1-10.

The World Bank. (2007). Dhaka: Improving living conditions for the urban poor. Sustainable Development Unit, South Asia Region, Report No. 35824-BD

Trotter, L., Dewan, A., & Robinson, T. (2017). Effects of rapid urbanisation on the urban thermal environment between 1990 and 2011 in Dhaka Megacity, Bangladesh. *AIMS Environmental Science*, *4*(1), 145-167.

Uejio, C. K., Wilhelmi, O. V., Golden, J. S., Mills, D. M., Gulino, S. P., & Samenow, J. P. (2011). Intra-urban societal vulnerability to extreme heat: the role of heat exposure and the built environment, socioeconomics, and neighborhood stability. *Health & place*, *17*(2), 498-507.

Weng, Q. (2001). A remote sensing-GIS evaluation of urban expansion and its impact on surface temperature in the Zhujiang Delta, China. *Int. J. Remote Sens*, *22*, 1999–2014.

Weng, Q., &Yang, S. (2004). Managing the adverse thermal effects of urban development in a densely populated Chinese city. *J. Environ. Manag*, 70, 145–156.

Weng, Q., Lu, D., & Schubring, J. (2004) Estimation of land surface temperature–vegetation abundance relationship for urban heat island studies. *Remote Sensing of Environment*, 89(4): 467–483.

Yow, D. M. (2007). Urban heat islands: observations, impacts, and adaptation. *Geography Compass*, *1*(6), 1227-1251.

Zha, Y., Gao, J., & Ni, S. (2003). Use of normalized difference built-up index in automatically mapping urban areas from TM imagery. *International journal of remote sensing*, *24*(3), 583-594.

Zhang X, Zhong T, Wang K, et al. (2009) Scaling of impervious surface area and vegetation as indicators to urban land surface temperature using satellite data. *International Journal of Remote Sensing* 30(4): 841–859.

Zhao, H., & Chen, X. (2005, July). Use of normalized difference bareness index in quickly mapping bare areas from TM/ETM+. In *International geoscience and remote sensing symposium*, *3*, *1666*.